

Solid FeS lubricant: a possible alternative to MoS₂ for Cu–Fe-based friction materials

Tao Peng, Qing-zhi Yan, Xiao-lu Zhang, and Xiao-jiao Shi

Laboratory of Special Ceramics and Powder Metallurgy, University of Science and Technology Beijing, Beijing 100083, China
(Received: 13 March 2017; revised: 23 June 2017; accepted: 25 June 2017)

Abstract: Molybdenum disulfide (MoS₂) is one of the most commonly used solid lubricants for Cu–Fe-based friction materials. Nevertheless, MoS₂ reacts with metal matrices to produce metal sulfides (e.g., FeS) and Mo during sintering, and the lubricity of the composite may be related to the generation of FeS. Herein, the use of FeS as an alternative to MoS₂ for producing Cu–Fe-based friction materials was investigated. According to the reaction principle of thermodynamics, two composites—one with MoS₂ (Fe–Cu–MoS₂ sample) and the other with FeS (FeS–Cu₂S–Cu–Fe–Mo sample), were prepared and their friction behaviors and mechanical properties were compared. The results showed that MoS₂ reacted with the Cu–Fe matrix to produce FeS, metallic ternary sulfides, and Mo when sintered at 1050°C. The MoS₂–Cu–Fe and FeS–Cu₂S–Cu–Fe–Mo samples thereby exhibited similar characteristics with respect to phase composition, density, hardness, and tribological behaviors. Micrographs of the worn surfaces revealed that the stable friction regime for both composites stemmed from the iron sulfides friction layers rather than from the molybdenum sulfides layers.

Keywords: friction materials; solid lubricants; iron sulfides; molybdenum sulfides

1. Introduction

Cu–Fe-based powder metallurgy (P/M) friction materials are now widely used in vehicle brake pads and industrial clutches because of their stable coefficient of friction (COF), good heat resistance, and high strength [1–5]. MoS₂ is one of the most commonly used solid lubricants for Cu–Fe-based friction materials; it can be used to stabilize friction and improve the wear resistance of composites [6–9]. However, numerous studies have shown that MoS₂ reacts with Cu or Fe matrices when sintered at temperatures above 950°C [10–21]; our recent study revealed that the lubricity of MoS₂ is attributable to the resultant formation of metal sulfides such as FeS [21]. Because of its layered structure, good thermal stability, and low cost, FeS may be a suitable alternative to MoS₂ lubricants in the production of Cu–Fe-based friction materials.

In this work, we investigated the use of FeS as an alternative to MoS₂ for Cu–Fe-based P/M friction materials. A sample with FeS (FeS–Cu₂S–Cu–Fe–Mo system, abbrevi-

ated FS) was designed to feature constituents consistent with the friction material containing MoS₂ (MoS₂–Cu–Fe system, abbreviated MS). The two samples were compared by phase analyses, microscopy observations, and tests of their mechanical and friction properties.

2. Experimental

2.1. Component design

The designed systems were MS and FS. MS embodied the common compositions of Cu–Fe-based braking materials, and FS served as a reference material for comparison. Fe (spherical), Cu (rod-shaped), MoS₂ (lamellar), FeS (irregular-shaped), Cu₂S (granular), and Mo (ellipsoidal) powders were used as the main ingredients in the experiments (Fig. 1). Given the accuracy of X-ray detection, 10wt% of MoS₂ was added to the MS system. The dosages of FeS and Cu₂S were selected on the basis of potential chemical reactions [19]. Detailed compositions are listed in Table 1.

Corresponding author: Qing-zhi Yan E-mail: qzyan@ustb.edu.cn

© The Author(s) 2017. This article is published with open access at link.springer.com

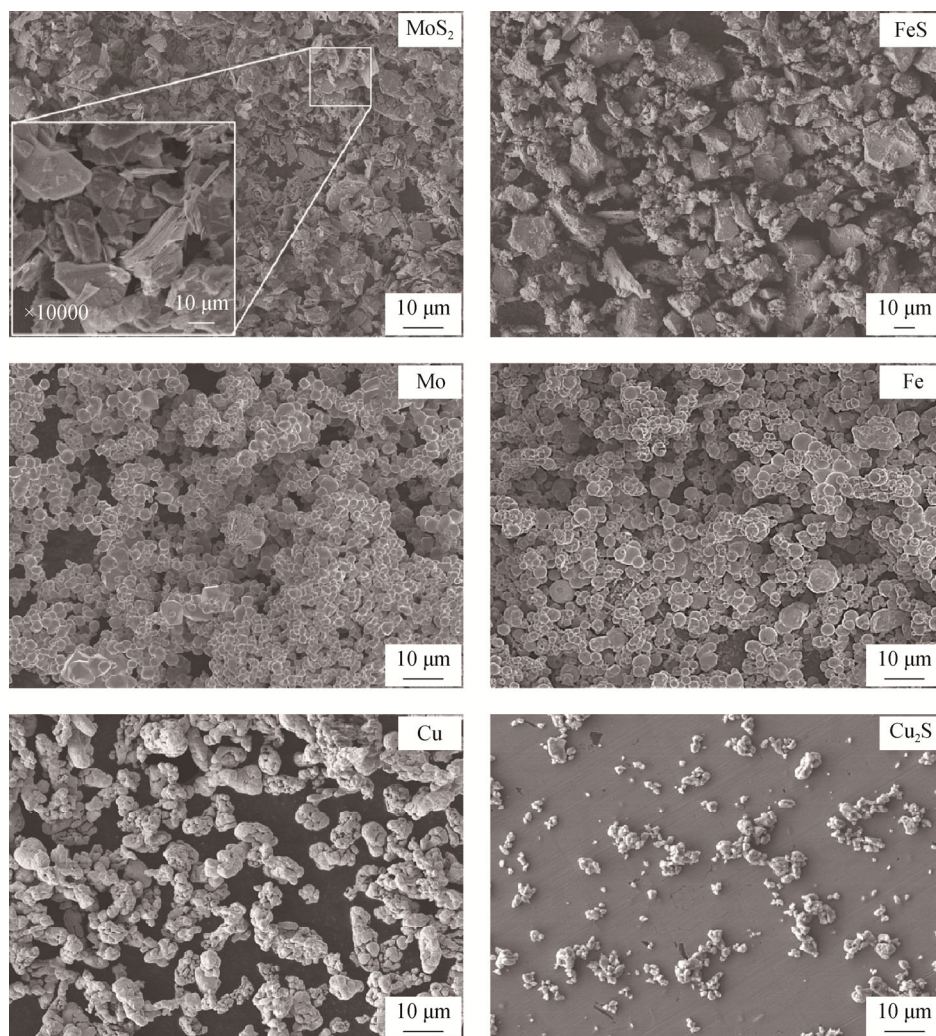


Fig. 1. SEM morphologies of the powders used in the experiments.

Table 1. Chemical composition of the samples wt%

Sample	MoS ₂	FeS	Cu ₂ S	Mo	Fe	Cu
MoS ₂ -Cu-Fe (MS)	10	—	—	—	45	45
FeS-Cu ₂ S-Mo-Cu-Fe (FS)	—	5.49	9.95	5.99	41.5	37.07

2.2. Sample preparation

All powders were well blended proportionally according to Table 1 in a V-type mixer for 2 h and then cold pressed under 300 MPa. The compacted samples were sintered at $(1050 \pm 5)^\circ\text{C}$ (the common sintering temperature for Cu–Fe-based composite materials) in a box furnace under a nitrogen–hydrogen ($\text{N}_2:\text{H}_2 = 3:1$ by volume) atmosphere for 30 min and were then cooled to room temperature.

2.3. Performance testing

X-ray diffraction (XRD) was used to analyze the phase

composition of the samples before and after sintering. Scanning electron microscopy (SEM) in conjunction with energy-dispersive X-ray spectrometry (EDS) was used to observe the microstructure of the samples and to analyze the constituents of the materials, respectively. The density and porosity of the sintered samples were measured by the Archimedes method. The hardness of samples was determined using a Vickers hardness tester (model MH-6) operated with a force of 200 N for 10 s. Compression strength was tested on a universal testing device (model WDW-50) using cylindrical specimens measuring $\phi 7.8 \text{ mm} \times 10 \text{ mm}$. The average result of five tests is reported in this work.

Dry sliding wear tests were carried out using a pin-on-disc testing device (Plint TE-92 multifunction friction tester); the pin and disc featured three-point contact. The disc was made of forged steel (30CrSiMoVA) with a hardness of HRC 55–60, a surface roughness of $0.05 \mu\text{m}$,

and a friction diameter of 60 mm. The sintered composite materials were cut into cylindrical pins with a diameter of (7.9 ± 0.1) mm and a height of (20 ± 0.2) mm. The dry sliding tests were carried out at a sliding speed of 0.94 m/s (300 r/min) under a normal pressure of 0.35 MPa and a total duration of 60 s. Before each test, the pins were abraded with the disc under a normal pressure of 0.28 MPa and a rotating speed of 300 r/min to ensure uniform contact with the disc. Because the wear tests were conducted under relatively mild conditions, the wear loss of the samples was minimal; the wear-loss results are therefore not described in the text.

3. Results and discussion

3.1. Phase analysis

The XRD patterns of the mixed powders and the sintered samples are shown in Figs. 2(a) and 2(b), respectively. All of the original components— MoS_2 , Mo, Fe, Cu, FeS, and Cu_2S , were detected in the powders before sintering (Fig. 2(a)). The peak intensity of a given powder depends on its concentration and degree of crystallinity, among other factors. In the as-sintered samples, no peak attributable to MoS_2 or Mo was observed in the pattern of either MS or FS. New peaks of phases such as FeS, CuFeS_2 , and $\text{Cu}_{1.84}\text{Mo}_6\text{S}_8$ were detected in the pattern of the as-sintered MS. Because MoS_2 cannot decompose under the sintering conditions used in this work [22], we speculated that MoS_2 reacted with Fe or Cu matrix to produce these complex sulfides and Mo. The presence of identical components in the patterns of as-sintered MS and FS confirmed this supposition. No Mo peak was observed in the pattern of either sample because of the partial dissolution of this element into the metal matrices [23], which will be discussed later.

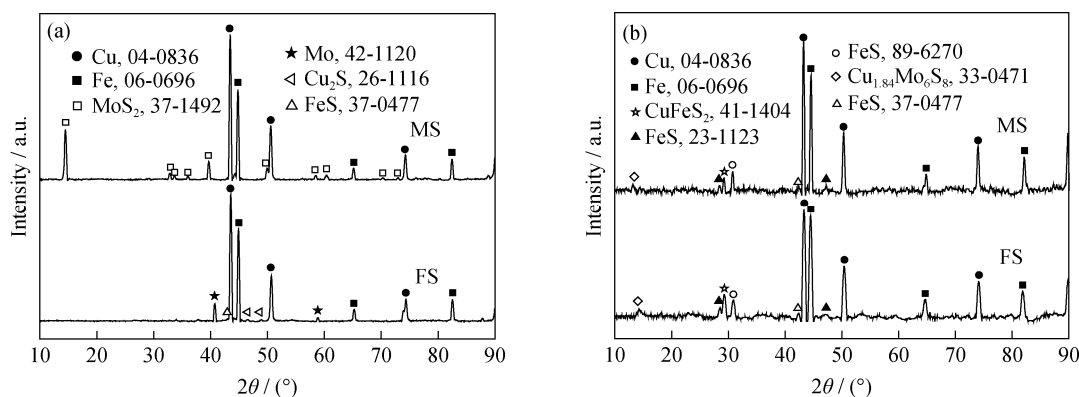


Fig. 2. XRD patterns of (a) the mixed powders and (b) the sintered products (the numbers in figure indicate the corresponding PDF Card numbers for different phases).

3.2. Microstructural analysis

Fig. 3 shows the backscattered electron (BSE) images of the sintered samples. Six regions, which are marked with different colors, are observed in the image of MS (Fig. 3(a)). On the basis of the corresponding EDS results, the gray regions represent Fe and the light-gray regions represent Cu.

The other three regions are assumed to be associated with the products of reactions between MoS_2 and the matrices. White particles represent Mo, which was produced during the sintering and distributed unevenly in the matrices. The particles represented by blue arrows consisted mainly of Fe and S in an atomic ratio of approximately 1 (Fig. 3(c)) according to the EDS analysis results. Combining these findings with the XRD results, we deduced that these regions were FeS and were preferentially located adjacent to Mo particles. The last regions (red arrows) were determined to contain Cu, Fe, S, and Mo; we therefore identified these regions as metallic ternary sulfides CuFeS_2 and $\text{Cu}_{1.84}\text{Mo}_6\text{S}_8$. These sulfides tended to locate at the border of Fe and Cu. Several pores (the sixth region) were also observed in the sample.

The compositions of the six regions in the BSE images of FS were identical to those in the BSE images of MS; however, each region in FS was finer and distributed more uniformly than the corresponding regions in MS. This finding is attributed to the inhibition of mutual contact between the particles as a result of the presence of more additives in the FS system.

3.3. Mechanical properties

The porosity (ε), density (ρ), compressive strength (σ), and Vickers hardness (HV) of the sintered samples are illustrated in Fig. 4. The FS displayed a higher porosity than

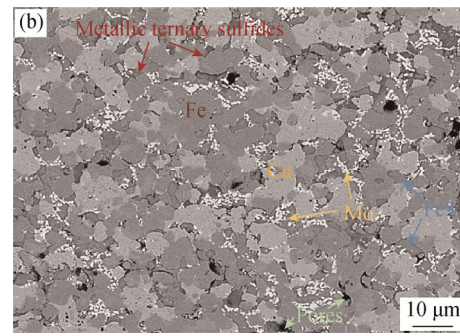
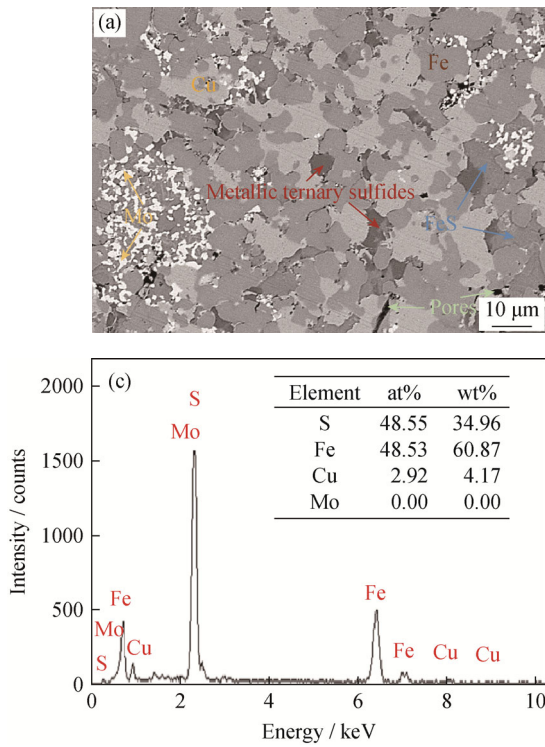


Fig. 3. Backscattered electron (BSE) micrographs of (a) the MS system and (b) the FS system (the main observed component phases are indicated); (c) the most representative EDS spectrum of the regions indicated by the blue arrows in (a) and (b) (5 points per sample).

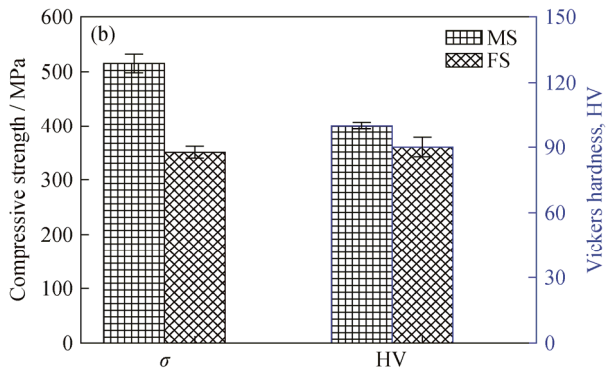
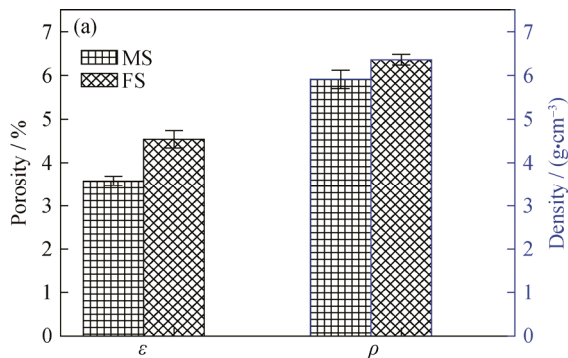


Fig. 4. Properties of the samples: (a) porosity (ϵ) and density (ρ); (b) compressive strength (σ) and Vickers hardness (HV).

MS as a result of the presence of more particle interfaces in the FS sample. The densities of the two samples were approximately equal. The MS exhibited a higher compressive strength than FS, whereas their Vickers hardnesses were approximately equal (Fig. 4(b)). These results indicate that FS exhibits micromechanical properties similar to those of MS, although FS exhibits inferior macromechanical properties because of its higher porosity. In addition, the reaction between MoS₂ and the matrices promotes the diffusion of Mo (from MoS₂ particles) into the iron matrix to form an Fe(Mo) solid solution, which reinforces the composites [24].

3.4. Comparison of friction behavior

The constant-speed COF of the samples is illustrated in Fig. 5. The initial sharp increases in the COF of both sam-

ples, where the COFs increase linearly until a normal pressure of 0.35 MPa is achieved, represent a loading stage. The COFs of both samples are nearly identical with respect to both the COF values and their fluctuation ranges (0.53–0.59).

To further explain the similarities in the COFs of the two systems, we obtained representative BSE images of the worn surfaces of the MS and FS specimens (Fig. 6). Notably, both samples' surfaces were covered with an integrated and continuous antifriction layer such that little of the matrix was observed. EDS analysis demonstrated that the layers of both samples had similar chemical compositions: Fe, Cu, S, O, and Mo, as shown in Fig. 7. Given the concentrations of these elements, the main components of these layers were assumed to be iron sulfides and oxides. Such sulfide and oxide coatings can be generated by the smear effect or by the oxidation of FeS and metallic ternary sulfides. The anti-

friction layer was found to be well adhered to the matrices and played an important role in preventing metal-on-metal contact during the rubbing process, thereby ensuring a stable and low COF. Consequently, we concluded that the two samples abide by the same friction mechanism and that the produced iron sulfides rather than the MoS_2 itself enhances the lubricity.

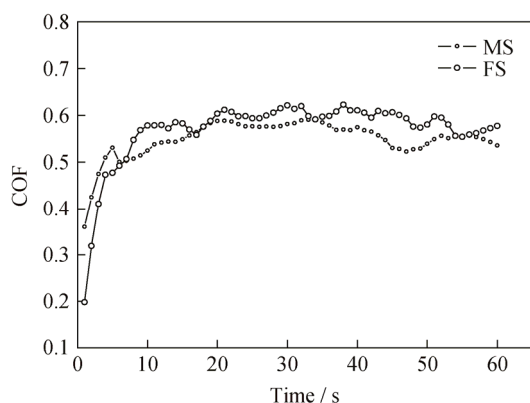


Fig. 5. Comparison of the coefficients of friction (COFs) of the sintered MS and FS systems under a normal pressure of 0.35 MPa.

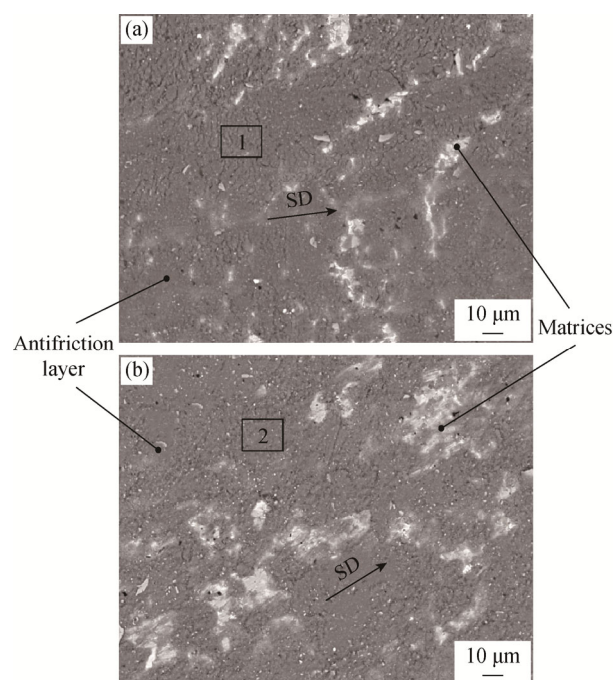


Fig. 6. SEM micrographs of the worn surfaces of (a) the MS system and (b) the FS system (black arrows indicate the sliding direction (SD)).

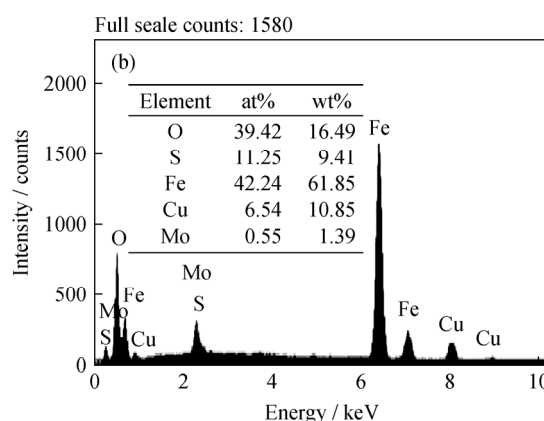
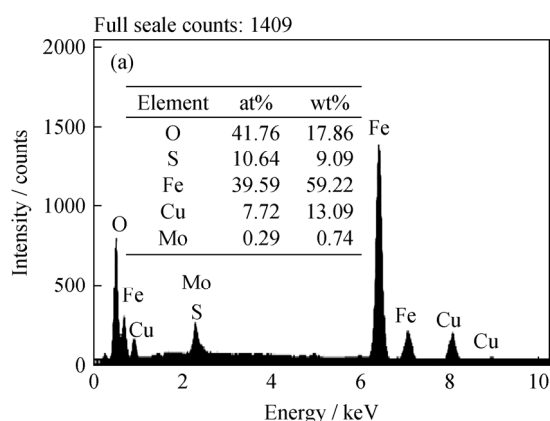


Fig. 7. EDS spectra of the friction layer captured in (a) box 1 in Fig. 6(a) and (b) box 2 in Fig. 6(b).

4. Conclusions

The use of FeS as an alternative to MoS_2 for Cu–Fe-based P/M friction materials was investigated. The two samples—MS and FS, were compared on the basis of phase analyses, microscopy observations, and tests of their mechanical and friction properties. The main conclusions deduced from the results of this study are summarized as follows:

(1) MoS_2 reacted with the Cu–Fe matrix under the sintering conditions to produce FeS, metallic ternary sulfides, and Mo. As a result, the phase compositions of the MS system are identical to those of the FS system.

(2) The MS displayed a lower porosity but higher com-

pressive strength than FS, whereas the densities and Vickers hardness of both samples were approximately equal.

(3) FeS and metallic ternary sulfides were uniformly distributed in the matrices for both the MS and FS systems. During the rubbing process, the worn surfaces of both samples were covered with an integrated and continuous antifriction layer, which led to their similar friction behaviors.

(4) The two samples abide by the same friction mechanism, and the lubricity benefits from the produced iron sulfides rather than from the MoS_2 itself. Given the high cost and lability of MoS_2 , FeS may be a desirable alternative to MoS_2 for producing Cu–Fe-based friction materials.

Acknowledgements

This work was financially supported by the National Natural Science Foundation of China (No. 51572026).

Open Access This article is distributed under the terms of the Creative Commons Attribution 4.0 International License (<http://creativecommons.org/licenses/by/4.0/>), which permits unrestricted use, distribution, and reproduction in any medium, provided you give appropriate credit to the original author(s) and the source, provide a link to the Creative Commons license, and indicate if changes were made.

References

- [1] R.M. German, *Powder Metallurgy and Particulate Materials Processing: The Processes, Materials, Products, Properties, and Applications*, Metal Powder Industries Federation, Princeton, 2005.
- [2] G.M. Zhang, K.Q. Feng, Y. Li, and H.F. Yue, Effects of sintering process on preparing iron-based friction material directly from vanadium-bearing titanomagnetite concentrates, *Mater. Des.*, 86(2015), p. 616.
- [3] T. Ram Prabhu, V.K. Varma, and S. Vedantam, Effect of reinforcement type, size, and volume fraction on the tribological behavior of Fe matrix composites at high sliding speed conditions, *Wear*, 309(2014), No. 1-2, p. 247.
- [4] W. Österle, C. Prietzel, H. Kloß, and A.I. Dmitriev, On the role of copper in brake friction materials, *Tribol. Int.*, 43(2010), No. 12, p. 2317.
- [5] X. Zhao, L.C. Guo, L. Zhang, T.T. Jia, C.G. Chen, J.J. Hao, H.P. Shao, Z.M. Guo, J. Luo, and J.B. Sun, Influence of nano-Al₂O₃-reinforced oxide-dispersion-strengthened Cu on the mechanical and tribological properties of Cu-based composites, *Int. J. Miner. Metall. Mater.*, 23(2016), No. 12, p. 1444.
- [6] A. Savan, E. Pflüger, P. Voumard, A. Schröer, and M. Simmonds, Modern solid lubrication: Recent developments and applications of MoS₂, *Lubr. Sci.*, 12(2000), No. 2, p. 185.
- [7] A. Erdemir, Review of engineered tribological interfaces for improved boundary lubrication, *Tribol. Int.*, 38(2005), No. 3, p. 249.
- [8] F.J. Clauss, *Solid Lubricants and Self-Lubricating Solids*, Elsevier, Amsterdam, 2012, p. 78.
- [9] M.H. Cho, J. Ju, S.J. Kim, and H. Jang, Tribological properties of solid lubricants (graphite, Sb₂S₃, MoS₂) for automotive brake friction materials, *Wear*, 260(2006), No. 7-8, p. 855.
- [10] S. Li, Y. Feng, S. Ling, X.B. Zhang, and J. Wang, Effect of sintering temperature on properties of Cu–MoS₂ composite materials, *Met. Funct. Mater.*, 15(2008), No. 1, p. 24.
- [11] D. Uzunsoy, E. Kelesoglu, and Y. Erarslan, Contribution of MoS₂ additives to the microstructure and properties of PM copper based brake material, *Mater. Test.*, 51(2009), No. 5, p. 318.
- [12] S. Dhanasekaran and R. Gnanamoorthy, Dry sliding friction and wear characteristics of Fe–Cu alloy containing molybdenum di sulphide, *Mater. Des.*, 28(2007), No. 4, p. 1135.
- [13] S. Dhanasekaran and R. Gnanamoorthy, Heat generation in Fe–Cu–MoS₂-sintered spur gears under unlubricated conditions, *Proc. Inst. Mech. Eng. Part J J. Eng. Tribol.*, 221(2007), No. 6, p. 645.
- [14] S. Dhanasekaran and R. Gnanamoorthy, Microstructure, strength and tribological behavior of Fe–Cu–Ni sintered steels prepared with MoS₂ addition, *J. Mater. Sci.*, 42(2007), No. 12, p. 4659.
- [15] H. Kato, M. Takama, Y. Iwai, K. Washida, and Y. Sasaki, Wear and mechanical properties of sintered copper–tin composites containing graphite or molybdenum disulfide, *Wear*, 255(2003), No. 1-6, p. 573.
- [16] K.P. Senthil, K. Manisekar, E. Subramanian, and R. Narayanasamy, Dry sliding friction and wear characteristics of Cu–Sn alloy containing molybdenum disulfide, *Tribol. Trans.*, 56(2013), No. 5, p. 857.
- [17] K.P. Furlan, C. Binder, A.N. Klein, and J.D.B. de Mello, Thermal stability of the MoS₂ phase in injection moulded 17–4 PH stainless steel, *J. Mater. Res. Technol.*, 1(2012), No. 3, p. 134.
- [18] K.P. Furlan, J.Z. de Assunção, G. Paz, C. Binder, and A.N. Klein, Sintering studies and microstructural evolution of Fe–MoS₂ mixtures, *Mater. Sci. Forum*, 802(2014), p. 415.
- [19] K.P. Furlan, P.B. Prates, T. Andrea dos Santos, M.V. Gouvêa Dias, H.T. Ferreira, J.B. Rodrigues Neto, and A.N. Klein, Influence of alloying elements on the sintering thermodynamics, microstructure and properties of Fe–MoS₂ composites, *J. Alloys Compd.*, 652(2015), p. 450.
- [20] J.S. Han, J.H. Jia, J.J. Lu, and J.B. Wang, High temperature tribological characteristics of Fe–Mo-based self-lubricating composites, *Tribol. Lett.*, 34(2009), No. 3, p. 193.
- [21] T. Peng, Q.Z. Yan, Y. Zhang, X.J. Shi, and M.Y. Ba, Low-cost solid FeS lubricant as a possible alternative to MoS₂ for producing Fe-based friction materials, *Int. J. Miner. Metall. Mater.*, 24(2017), No. 1, p. 115.
- [22] Y. Wang, Q.Z. Yan, F.F. Zhang, C.C. Ge, X.L. Zhang, and H.Q. Zhao, Sintering behavior of Cr in different atmospheres and its effect on the microstructure and properties of copper-based composite materials, *Int. J. Miner. Metall. Mater.*, 20(2013), No. 12, p. 1208.
- [23] P.R. Subramanian, L. Kacprza, and W.W. Scott, *Binary Alloy Phase Diagrams*, American Society for Metals, Metals Park, OH, 1986.
- [24] J. Chen, P. Yao, and X. Xiong, The behaviors of MoS₂ in the sintering process of Fe-based friction materials, *Non Met. Mines*, 26(2003), No. 4, p. 50.